Abdelhadi NAMOUNE[1], Rachid TALEB[2], Ahmed DERROUAZIN[2], Abdelkader BELBOULA[2] and Azzedine HAMID[3]

Electrical Engineering Department, Institute of Sciences and Technology, Ahmed Zabana University Centre, Relizane, Algeria (1),
Electrical Engineering Department, Hassiba Benbouali University, LGEER Laboratory, Chlef, Algeria (2),
Electrical Engineering Department, USTO-MB University, Laboratory of Integration for Power Electronics & Materials, Oran, Algeria (3)

doi:10.15199/48.2019.09.11

Integrated square shape inductor with magnetic core in a buck converter DC-DC

Abstract. *This paper presents the buck converter DC-DC. At first, we define the characteristics of the converter. The second, we descript our inductor; the topology of square shape inductor has been presented to extract the geometric parameters. The equivalent electrical model approved of the integrated inductor with magnetic core takes into account all the technological parameters which are illustrated by analytic expressions. Moreover, the results of different simulations concern the effect of geometrical parameters of inductor on the inductance value and quality factor. Finely, we performed simulations on the operating of our buck converter including firstly an ideal inductor and then an integrated inductor with magnetic core. Simulation results have shown that the waveforms of the current and output voltage in both cases are similar.*

Streszczenie. *Zaprezentowano przekształtnik typu buck DC-DC wykorzystujący planarną indukcyjność. Przedstawiono analiz wpływu wymiarów dławika na parametry indukcyjności takie jak dobroć.* ***Przekształtnik DC_DC ze scalonym planarnym dławikiem***

Keywords: inductor, magnetic core, integration, buck converter, geometric parameters.
Słowa kluczowe: dławik planarny, przekształtnik typu buck

Introduction

The always-augmenting demand for multifunctional and undersize portable electronic devices is driving the improvement of miniaturized DC-DC converters [1 – 3]. Such converters are used to shift voltage levels in electronic systems with high efficiency. There are multiple applications for such converters. For example, state-of-the-art portable smart phones and tablet PCs feature multiple components, such as the display panel, MEMS sensors, data storage devices, and cameras, which may require different operating voltage levels. Miniaturizing these converters reduces the overall size of the portable devices [4].

Passive components are the major factor in determining the overall size, cost and performance of portable products. The drive to further miniaturization and integration of portable electronic devices has recently focused on the task of passive functions [5, 6].

Integration of passive devices in the same silicon substrate is desirable in order to reduce this interconnect parasitic, reduce the size and cost of the units and increase the operating frequencies of the radio frequency circuits. Inductors are elementary and important parts in radio frequency integrated circuits [7, 8].

In this paper, the behavior of inductor is systematically studied and the impact of the geometrical parameters on its inductance and quality factor. The principal object of my paper is to detail all the phases of design and modeling of square shape inductor in order to attain its simulation and integrate it into a buck converter. This power inductor with magnetic core increases the quality factor value while reducing the constituent dimensions with a small manufacturing cost.

Buck converter DC-DC

The buck converter circuit is shown in figure 1. The switch *T* has a duty cycle *D* which ranges from 0 to 1. Figure 2 indicates relevant waveforms of the circuit when the switch *T* is turned *ON* and *OFF* at frequency *f*, with a duty cycle *D* [9].

The design specifications of buck converter with an output power of 0.6 W are enlisted in Table 1 and Table 2:

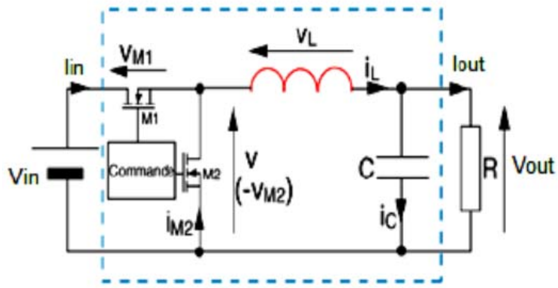

Fig. 1. Schematic of a typical DC-DC buck converter

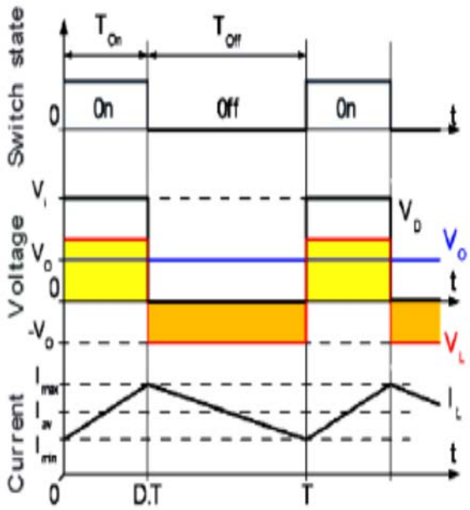

Fig. 2. Waveforms of the voltages and currents with time in a buck converter

The following equations then hold for the buck converter [10].

(1) $$I_{out} = \frac{P_{out}}{V_{out}}$$

(2) $$D = \frac{V_{out}}{V_{in}}$$

(3) $$L = \frac{(V_{in} - V_{out}).D}{2.\Delta I_L.f}$$

Table 1. Principal specification

Specifications	Symbol	Value
Output Power	P_0	0.6 W
Input Voltage	*Vin*	7
Output Voltage	*Vout*	2.4
Frequency	*f*	5 MHz

Table 2. Material specification

Elements	Material	Characteristics
Conductor	Copper (Cu)	Resistivity : $\rho_{Cu} = 1.7 \times 10^{-8}$ [Ω.m] Conductivity : $\sigma_{Cu} = 5.8 \times 10^{7}$ [S/m]
Oxide	Silicon dioxide (SiO_2)	permittivity : $\varepsilon_{ox} = 3.97\ \varepsilon_0$ $\varepsilon_0 = 8.85 \times 10^{-12}$ [F/m]
Substrate	Silicon (Si)	Resistivity : $\rho_{Si} = 2.27 \times 10^{-1}$ [Ω.m] Permittivity : $\varepsilon_{Si} = 11.9\ \varepsilon_0$
magnetic core	Ferrite (NiFe)	Resistivity : $\rho_{NiFe} = 20 \times 10^{-8}$ [Ω.m]

Topology and dimensions inductor

Figure 3 illustrates a power inductor in silicon with a single spiral winding layer and two electroplated magnetic core layers. From the schematic 3D view in Figure 3(a), the spiral windings are capped by two magnetic plates. From the cross-section view in Figure 3(b), the copper windings and magnetic vias are embedded into the silicon substrate [11][12][13].

a)

b)

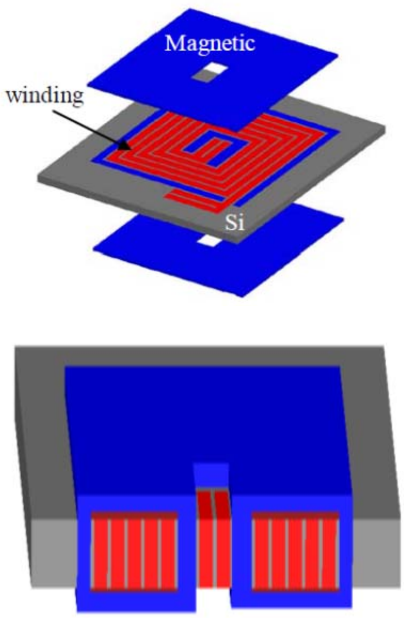

Fig. 3. (a) Schematic 3D view, (b) Cross-section view of a power inductor

In radio-frequency integrated circuits, inductor of square shape is used for this design, as shown in Figure 4. The geometry parameters of the spiral inductor are the number of turns *n*, the width of the metal trace *w*, the turn spacing *s*, the thickness of conductor *t*, the inner diameter *din* and the outer diameter *dout* [14].

The fill ratio (α) is given by either of the following expression [15]:

(4) $$\alpha = \frac{d_{out} - d_{in}}{d_{out} + d_{in}}$$

The average diameter of inductor given by [16]:

(5) $$d_{avg} = \frac{d_{out} + d_{in}}{2}$$

To calculate the width of the conductor and the thickness of conductor, it is obligatory to complete the next condition [17]:

(6) $$w \le 2\delta \quad \text{or} \quad t \le 2\delta$$

where *δ* is the skin depth expressed by [17]:

(7) $$\delta = \sqrt{\frac{1}{\pi.f.\sigma_{cu}}}$$

The spacing between conductors is articulated by [18]:

(8) $$s = \frac{d_{out} - d_{in} - 2.w.n}{2(n-1)}$$

The length of the winding conductor in a square shape inductor is construed from the relation [19]:

(9) $$l = 4.n.[d_{out} - (n-1).s - n.w] - s$$

Table 3 contains the specifications and the design results of the square shape inductor.

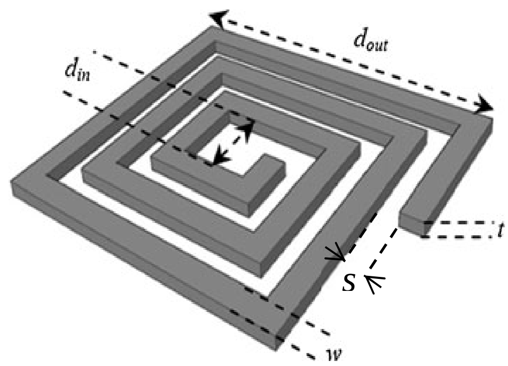

Fig. 4. Layout of a square shape inductor

Table 3. The geometrical parameters of the square spiral inductor

Geometric parameters	Symbol	Value
Number of turns	*n*	3
Spacing between turns	*s*	7 µm
Width of conductor	*w*	18 µm
Thickness of conductor	*t*	1,5 µm
Inner diameter	*din*	70 µm
Outer diameter	*dout*	206 µm
Total length	*l*	1,64 mm

Extraction technological parameter

The cross-section of a spiral inductor together with its equivalent π model is illustrated in Figure 4 (a) and (b) [20]. *Ls* consist of the self-inductance, positive mutual inductance, and negative mutual inductance. *Cs* is the capacitance between metal lines. *Rs* is the series resistance of the metal line. *Cox* is the capacitance of oxide layer underneath the spiral. *Rsub* and *Csub* are the coupling resistance and capacitance associated with silicon substrate. *Rmag* represent the ohmic losses in the magnetic core (ferrite).
Where, the thickness of substrate silicon (t_{sub}= 50 µm), the thickness of ferrite NiFe (t_{mag}= 31 µm) and thickness of the oxide of silicon SiO2 (t_{ox}= 23 µm).

These technological parameters can be roughly calculated using the formulas [21] [22], listed in Table 4, which would serve as starting point of simulation.

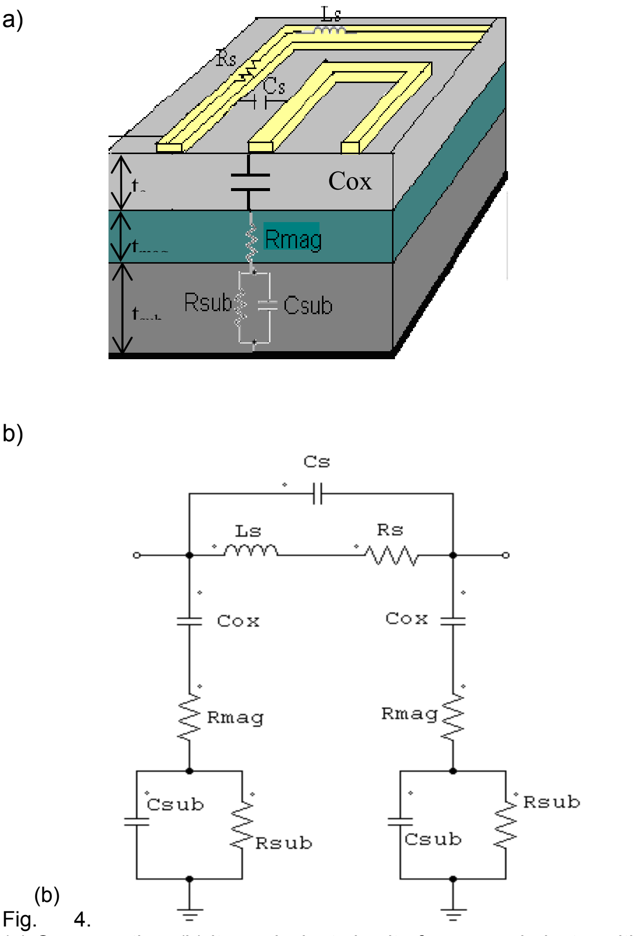

Fig. 4.
(a) Cross-section, (b) its equivalent circuit of a square inductor with magnetic core [20]

Table 4. Formulas and results for technological parameters

Symbol	Analytical equation	Value
Ls	$\dfrac{(2,34.\mu_0.n^2.d_{avg})}{(1+2,75.\alpha)}$	1,55 nH
Rs	$\dfrac{1}{w.\sigma.\delta.(1-e^{-t/\delta})}$	28,9 KΩ
Cs	$\dfrac{n.w^2.\varepsilon_{ox}}{t_{ox}}$	1,484 fF
Cox	$\dfrac{w.l.\varepsilon_{ox}}{2.t_{ox}}$	0,022 pF
Rmag	$\dfrac{2.\rho_{NiFe}.t_{mag}}{l.w}$	0,42 mΩ
Rsub	$\dfrac{2.\rho_{si}.t_{sub}}{l.w}$	768,97 Ω
Csub	$\dfrac{\varepsilon_{si}.l.w}{2.t_{sub}}$	31,08 fF

Result and discussion

Effects of the inductor geometrical parameters

The square shape inductor has been simulated in the frequency range of 1MHz to 10 MHz by varying the geometrical parameters such as the number of turns *n*, the inner diameter *din*, width of conductor *w* and space between bordering turns *s*. In addition, their effects on the inductance *L* and quality factor *Q*. The results using geometric parameters give some insights on the simulated results obtained from the *MATLAB* software.

Number of turns

The inductance *L* and quality factor *Q* values related to frequency are illustrated in Figure 5 and Figure 6. As number of turns of the winding *n* varies from 2 to 4, the inductance value increases, while the quality factor decreases with frequency.

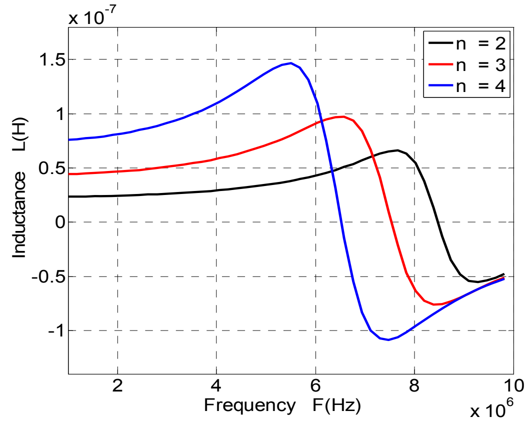

Fig. 5. Effect on inductance *L* for different number of turns

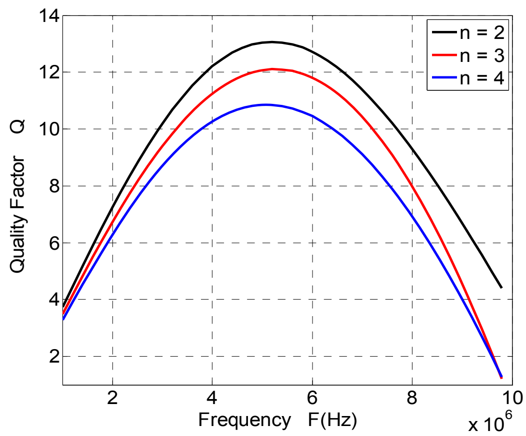

Fig. 6. Effect on quality factor *Q* for different number of turns

Inner diameter

Figure 7 shows how the inductance *L* changes with respect to frequency. As inner diameter *din* varies at (60 μm, 70 μm and 80 μm), *L* improves due to the increase in the length of conductor *l*. However, as inner diameter decreases, *Q* increases gradually, as shown in Figure 8. This increase is related to the distance between opposite sides at the center of the spiral.

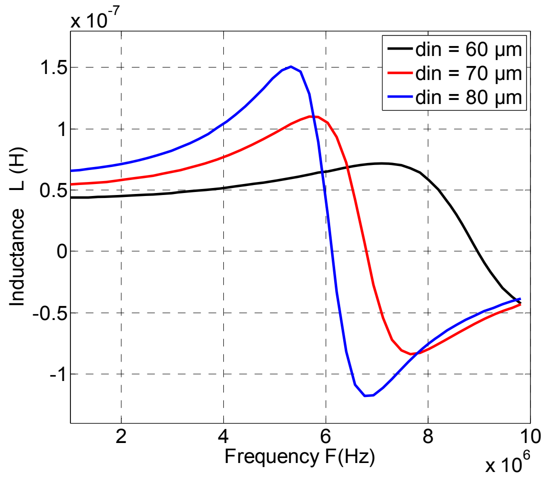

Fig. 7. Effect on inductance *L* for different inner diameter

Width of conductor

The width of conductor *w* is varied at (16 μm, 18 μm and 20 μm). Figure 9 show that *L* decreases slightly as *w* increases. In additions, as *w* increases, the penalty on the resistance due to the skin effect will dominate at a given frequency, hence, the quality factor *Q* shifts to a lower frequency, as indicated in Figure 10.

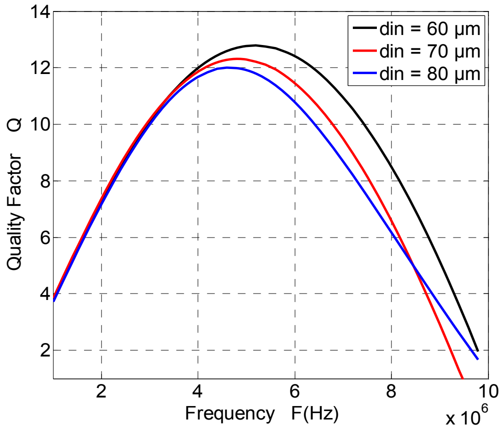

Fig. 8. Effect on quality factor *Q* for different inner diameter

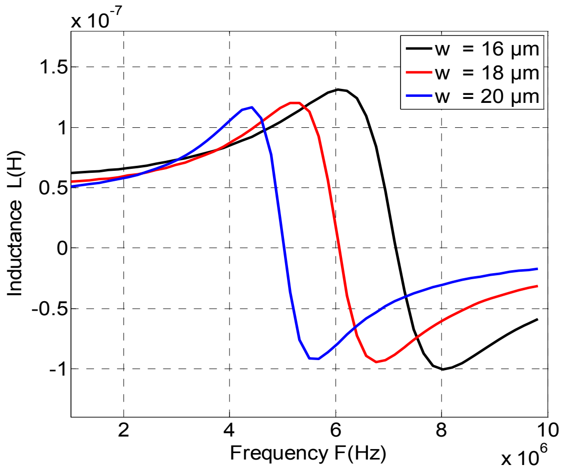

Fig. 9. Effect on inductance *L* for different width of conductor

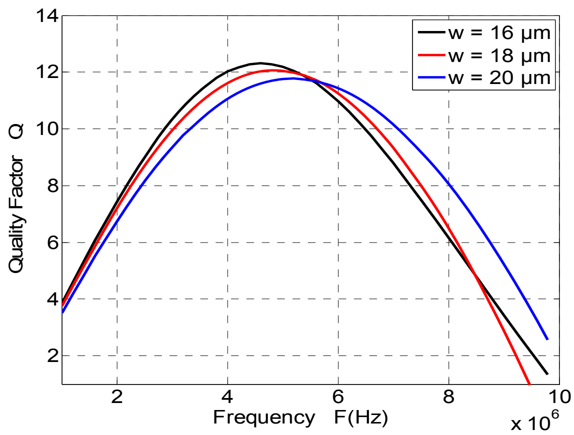

Fig. 10. Effect on quality factor *Q* for different width of conductor

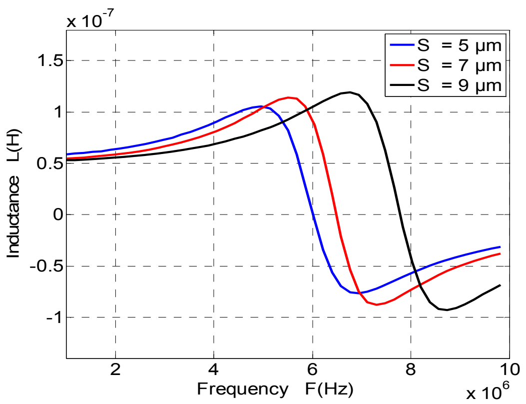

Fig. 11. Effect on inductance *L* for different spacing between windings

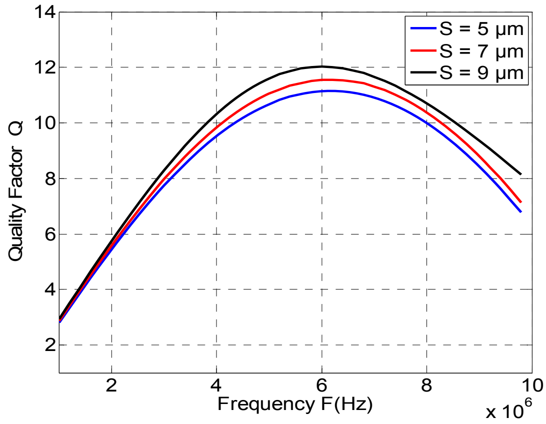

Fig. 12. Effect on quality factor *Q* for different spacing between windings

Spacing between turns

The influences of varying the separation distance between the windings *s*, from 5 µm to 9 µm. The inductance value decreases with increasing *s*. smaller separation distances result in higher capacitive coupling between the windings and therefore a lower self-resonance frequency. The quality factor value increases with increasing the distance between windings. The simulation results are shown in Figures 11 and 12.

Application of the buck converter

In this part, we present the results of simulation of the buck converter in two cases: ideal inductor and integrated inductor with magnetic core. We used for this paper the *PSIM* software.

Buck converter including ideal inductor

The circuit of Figure 13 contains an ideal inductor of the buck converter; Figure 14 shows the waveform of the output voltage and current of the buck converter.

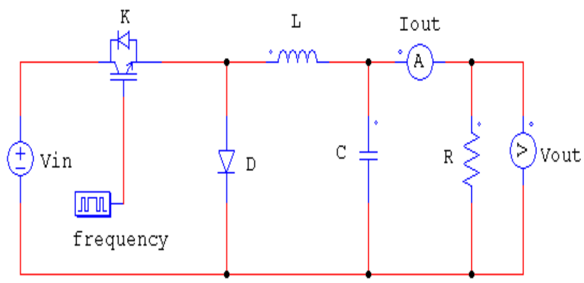

Fig. 13. buck converter with ideal inductor

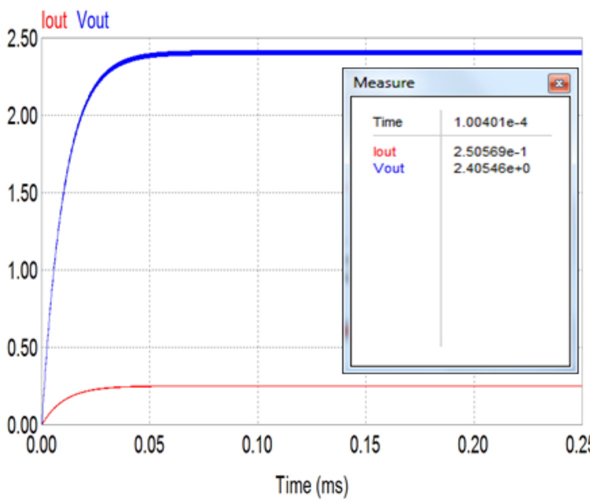

Fig. 14. Output voltage and current of the buck converter with ideal inductor

Buck converter including integrated inductor with magnetic core

Figure 15 shows the change ideal inductor of the buck converter by integrated inductor with magnetic core. The different technological parameters of the equivalent electrical models are calculated in Table 4. The Figure 16 shows the waveform of the output voltage and current of the buck converter.

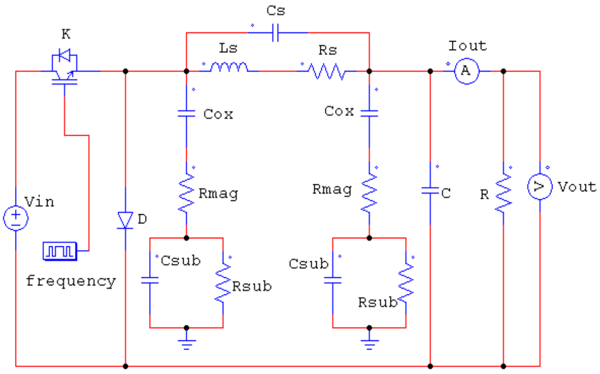

Fig. 15. buck converter with integrated inductor with magnetic core

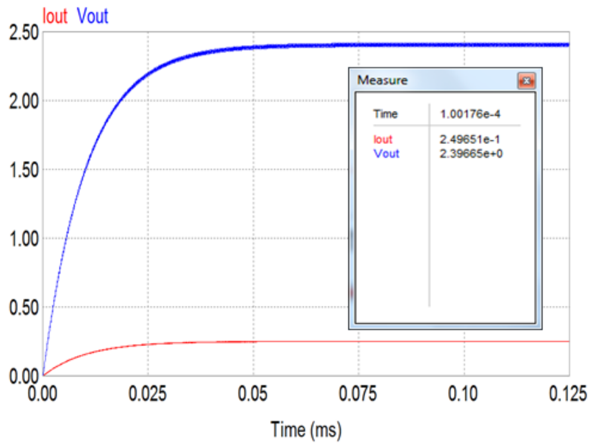

Fig. 16. Output voltage and current of the buck converter with integrated inductor with magnetic core

Conclusion

In this paper, we have presented the design and modeling of square shape inductor integrated in buck converter. The most difficult problem is to determine the geometrical and technological parameters of the inductor with magnetic core. Next, the geometry of square shape inductor is important and gives huge impact to the performance of radio-frequency integrated circuits. Indeed, the simulation of the quality factor of a square shape inductor topology requires both weakly the width of conductor, inner diameter and the number of turns. Finally, by using a software simulation *PSIM*, we have compared the waveforms of the buck converter output voltages and current for the two simulations (ideal inductor, integrated inductor with magnetic core). We remark the equivalent result between two cases.

***Corresponding author: Abdelhadi NAMOUNE**, Electrical Engineering Department, Institute of Sciences and Technology, Ahmed Zabana University Centre, Relizane, Algeria, Email: namoune.abdelhadi@gmail.com*

REFERENCES

[1] Johnson B., Pike G.E., Preparation of Papers for Transactions, *IEEE Trans. Magn.*, 50 (2002), No. 5, 133-137

[1] Lopez-Villegas J.M, Samitier J, Bausells J, Merlos A, Cané C, Knochel R, Study of integrated RF passive components performed using CMOS and Si micromachining technologies. *J Micromech Microeng*. Vol. 7, (1997), 162–164

[2] Burns L. M., Integrated circuit technology options for RFIC'spresent status and future directions. *IEEE J Solid State Circuits*. Vol. 33, (1998), 387–399

[3] Namoune A, Hamid A, Taleb R., Stacked transformer: influence of the geometrical and technological parameters. *International Journal of Engineering Research in Africa*, Vol. 21, (2015), No. 4, 148-164

[4] Ribas RP, Lescot J, Leclercq J-L, Karam JM, Ndagijimana F., Micro-machined microwave planar spiral inductors and transformers. *IEEE Trans Microw Theory Tech*, Vol. 48, (2000), No. 8, 1326–1326.

[5] Lu H-C, Chan TB, Chen CC-P, Liu C-M, Hsing H-J, Huang P-S., LTCC spiral inductor synthesis and optimization with measurement verification. *IEEE Trans Adv Packag*. Vol. 33, (2010), No. 1, 160–168.

[6] Melati R, Hamid A, Thierry L, Derkaoui M., Design of a new electrical model of a ferromagnetic planar inductor for its integration in a micro-converter. *Math Comput Model*. Vol. 57, (2013), No. 3, 200– 227

[7] BENJAMIN VALLET., Étude et conception d'une nouvelle alimentation à découpage à transfert d'énergie mixte basée sur un composant passif LCT intégré. *Université Joseph Fourier* (2008)

[8] Namoune A, Hamid A, Taleb R., the Performance of the Transformer for an Isolated DC/DC Converter. *TELKOMNIKA*, Vol. 15, (2017), No 3, 1031-1039

[9] Mohan N., Undeland T. M., and Robbins W. P., Power Electronics: Converters, Applications and Design, *3rd Edition*, 2003 Wiley.

[10] Wibben J. and Harjani R., A High-Efficiency DC-DC Converter Using 2 nH Integrated Inductors, *IEEE Journal of Solid-State Circuits*, Vol. 43, (2008),. 844-854

[11] Wang M., Batarseh I., Ngo K. D. T., and Xie H., Design and Fabrication of Integrated Power Inductor Based on Silicon Molding Technology, *Conference in Power Electronics Specialists, PESC 2007, IEEE*, (2007), 1612-1618

[12] Hayashi Z., Katayama Y., Edo M., and Nishio H., High-efficiency dc-dc converter chip size module with integrated soft ferrite, *IEEE Transactions on Magnetics*, Vol. 39, (2003), 3068-3072

[13] Ludwig M., Duffy M., O'Donnell T., McCloskey P., and Mathuna S. C. O., PCB integrated inductors for low power DC/DC converter, *IEEE Transactions on Power Electronics*, Vol. 18, (2003), 937-945

[14] Yue, P., and Wong, S. S., Physical modeling of spiral inductors on silicon. *IEEE Transactions on Electron Devices*, Vol. 47, (2000), No. 3, 560–568.

[15] Sia C. B., et al., Metallization Proximity Studies for Copper Spiral Inductors on Silicon, *IEEE Transaction on Semiconductor Manufacturing*, Vol. 16, (2003), No. 2

[16] Namoune A, Hamid A, Taleb R., Simulation Analysis of Geometrical Parameters of Monolithic On chip Transformer on Silicon Substrates. *Przeglad Elektrotechniczny*, Vol 93, (2016) No 1, 253-257, 2016

[17] Melati R., Hamid A., Thierry L., Modeling and dimensioning of a planar inductor for a monolithic integration, *Conference in: Asia-Pacific Power and Energy Engineering, IEEE Xplore*, (2011), 1–9.

[18] Nigam M. and Sullivan C. R., Multi-layer folded high-frequency toroidal inductor windings, *Conference and Exposition in Applied Power Electronics, APEC 2008. Twenty-Third Annual IEEE*, (2008), 682-688.

[19] Nguyen N., Ng K., Boellaard E., Pham N., Craciun G., Sarro P., and Burghartz J., Through-Wafer Copper Electroplating for RF Silicon Technology, *Conference in Solid-State Device Research, Proceeding of the 32nd European*, (2002),. 255-258.

[20] Yamaguchi M., Kuribara T., Arai K-I, Two port type ferromagnetic RF integrated inductor, *IEEE International Microwave Symposium (Seattle USA) (IMS-2002) TU3C-2*, (2002), 197-200

[21] Cao, Y., Groves, R. A., Huang, X., Zamdmer, N. D., Plouchart, J. O., Wachnik, R. A., et al., Frequency-independent equivalent-circuit model for on-chip spiral inductors. *IEEE Journal of Solid-State Circuits*, Vol. 38, (2003), No.3, 419–426.

[22] Koutsoyannopoulos, Y. K., & Papananos, Y., Systematic analysis and modeling of integrated inductors and transformers in RF IC design. *IEEE Transactions on Circuits and Systems-II: Analog and Digital Signal Processing*, 47, (2000), 699–713.